

TUNING OF KALMAN FILTER NOISE PARAMETERS FOR UNCERTAINTY QUANTIFICATION IN INPUT-STATE ESTIMATION OF MDOF SYSTEMS

**Marios Panias¹, Luigi Caglio¹, Sebastian T. Glavind², Amirali Sadeqi¹, Michael Havbro
Faber², Henrik Stang¹, and Evangelos Katsanos¹**

¹Department of Civil and Mechanical Engineering, Technical University of Denmark, Kgs. Lyngby,
2800, Denmark
e-mail: mariospanias@gmail.com, lucag@dtu.dk, vakat@dtu.dk, amisa@dtu.dk

²Department of the Built Environment, Aalborg University, Aalborg, Denmark

Abstract

The current research work deals with uncertainty quantification aspects in the problem of joint input-state estimation in structural dynamics. Specifically, it focuses on methodologies that can facilitate the tuning of the noise covariance matrices within the framework of Bayesian filtering techniques. These covariance matrices reflect the uncertainties of the estimation scheme and their proper calibration can reinforce the reliability of the estimated dynamic response. In this work, the performance of two approaches is investigated in the case of linear systems. First, a state-of-the-art methodology from the literature called Bayesian Expectation Maximization is implemented. The purpose of this optimization scheme is to identify the optimal noise covariance matrices based on the available observations of the dynamic response quantities. After evaluating the performance of this methodology, an adaptive time-varying noise Augmented Kalman Filter is proposed for updating the noise characteristics. The proposed scheme is expected to reduce the uncertainty of the input-state estimation. The two methods are applied on a 2D multi-story and multi-bay steel moment resisting frame subjected to earthquake-induced ground excitation. The performance of the different methods is evaluated and discussed.

Keywords: Augmented Kalman Filter, Input-state estimation, Uncertainty quantification, MDOF systems, Noise calibration

1 INTRODUCTION

Civil structures can be exposed to environmental or human-induced dynamic loads that may adversely affect their safety, serviceability, and remaining lifetime. Hence, the deployment of Structural Health Monitoring (SHM) campaigns is highly relevant for structural integrity management purposes. Along these lines, numerous studies in the field of vibration-based monitoring have pursued the extraction of information about structural performance remotely, using responses measured during operational conditions and extreme events. Specifically, the recovery of the full-field dynamic response of a structure, even in unmonitored or inaccessible locations, based on sparse noisy output-only measurements, has recently attracted growing interest in both the scientific community and industry.

Although Bayesian filtering techniques, such as Kalman-type filters, have been proven efficient tools for addressing the joint input-state estimation of linear [1-3] and nonlinear dynamical systems [4,5], the calibration of the filter-related parameters remains a cumbersome task. These parameters are the assumed measurement and process noise covariance levels, which reflect the uncertainties related to the entire estimation scheme, including the measurement uncertainty as well as the digital model's uncertainty. These sources of uncertainty can propagate to the estimation scheme undermining its accurate performance. While the measurement noise is directly related to the accuracy of the employed physical sensors, the process noise can act as a buffer for the model deficiency and reinforce the reliability of the estimated response. Slight variations in these covariance matrices might adversely affect the estimation results and lead to significant uncertainties in the estimations. Since these predictions form the basis for monitoring-driven decision-making, the quantification of those uncertainties is of high importance [6].

In the absence of expert knowledge, a trial-and-error approach or a heuristic rule of thumb are often adopted to tune the noise covariance matrices prior to the implementation of the filter [3]. This may not be possible when limited a-priori knowledge about the input and/or the states of the system is available. In such cases, an offline tuning phase is commonly employed, for example, by adopting the popular L-curve regularization procedure [1,2]. However, this procedure when implemented in connection with the Augmented Kalman Filter (AKF) for joint input-state estimation generates a curve that does not have a perfect L-shape, thereby rendering the selection of the noise parameters user-dependent [7].

Within this context, the current research work focuses on the identification of the Kalman Filter noise covariance matrices and the corresponding benefit in terms of improving the mean estimation as well as reducing the associated uncertainty when performing the joint input-state estimation of linear dynamical systems. Whilst updating of the noise parameters has been accomplished in some studies [8-10], posterior uncertainties were often ignored and the focus was mainly on improving the mean estimation. To this end, Teymouri et al. have established a fully Bayesian formulation and a novel Expectation-Maximization (*EM*) algorithm to update the noise covariance matrices iteratively in an offline fashion while focusing on the joint input-state estimation in linear systems [11]. Their methodology, abbreviated as BEM, can be regarded as an expanded version of the AKF, which allows for uncertainty quantification and propagation. An extended version of BEM has been proposed in [12], which utilizes BEM for the uncertainty quantification and propagation in coupled input-state-parameter-noise identification problems.

However, despite recent advances, there is a gap in uncertainty quantification and propagation for joint input-state estimation problems, demanding further research in this direction [11]. Hence, an adaptive noise methodology is proposed in this work, anticipated to address uncertainty quantification aspects in the joint input-state estimation of linear systems. In this approach, the AKF noise parameters are considered to be time-variant, accounting for changes in the modeling uncertainty and the dynamics of the unknown load. The performance of this

framework is assessed via a numerical example and the results are compared to those obtained by utilizing the state-of-the-art BEM methodology [11]. The proposed method is similar to [8] as both methods consider an adaptive noise scheme to address joint input-state estimation through the AKF. However, these contributions are entirely different in terms of mathematical formulation and uncertainty quantification scopes.

2 THEORETICAL BACKGROUND

The theoretical background and the mathematical formulation employed herein is presented below. First, the state-space formulation of a linear dynamical system is briefly introduced, followed by its implementation within the AKF for joint input-state estimation. For the sake of brevity, only the main equations are provided and more details can be found in [7].

2.1 State-Space formulation for linear systems

For a linear time-invariant dynamical system of n Degrees of Freedom (DOFs), the equation of motion reads:

$$\mathbf{M}\ddot{\mathbf{y}}(t) + \mathbf{C}\dot{\mathbf{y}}(t) + \mathbf{K}\mathbf{y}(t) = \mathbf{f}(t) = \mathbf{S}_p\mathbf{p}(t) \quad (1)$$

where \mathbf{M} , \mathbf{C} , and $\mathbf{K} \in \mathbb{R}^{n \times n}$ are the mass, damping and stiffness matrix, respectively; $\mathbf{f}(t) \in \mathbb{R}^n$ is the external input, while $\ddot{\mathbf{y}}(t)$, $\dot{\mathbf{y}}(t)$ and $\mathbf{y}(t) \in \mathbb{R}^n$ are the acceleration, velocity and displacement vectors, respectively. The external input $\mathbf{f}(t)$ can be written as the superposition of m load time histories $\mathbf{p}(t) \in \mathbb{R}^m$ multiplied with the influence matrix $\mathbf{S}_p \in \mathbb{R}^{n \times m}$. From Eq. (1), the following state space formulation in discrete time can be derived:

$$\mathbf{z}_{k+1} = \mathbf{A}\mathbf{z}_k + \mathbf{B}\mathbf{p}_k \quad (2)$$

$$\mathbf{d}_k = \mathbf{H}\mathbf{z}_k + \mathbf{J}\mathbf{p}_k \quad (3)$$

where $\mathbf{z}_k = [\mathbf{y}_k \ \dot{\mathbf{y}}_k]^T$ is the state vector, \mathbf{d}_k is the measurement vector, $\mathbf{A} = e^{\mathbf{A}_c \Delta t}$, Δt is the sampling period, $\mathbf{B} = [\mathbf{A} - \mathbf{I}]\mathbf{A}_c^{-1}\mathbf{B}_c$, $\mathbf{A}_c = [\mathbf{0} \ \mathbf{I}; -\mathbf{M}^{-1}\mathbf{K} \ -\mathbf{M}^{-1}\mathbf{C}]$, $\mathbf{B}_c = [\mathbf{0}; \mathbf{M}^{-1}\mathbf{S}_p]$, $\mathbf{J} = [\mathbf{0}; \mathbf{0}; \mathbf{S}_a\mathbf{M}^{-1}\mathbf{S}_p]$, $\mathbf{H} = [\mathbf{S}_d \ \mathbf{0}; \mathbf{0} \ \mathbf{S}_v; -\mathbf{S}_a\mathbf{M}^{-1}\mathbf{K} \ -\mathbf{S}_a\mathbf{M}^{-1}\mathbf{C}]$, \mathbf{I} is the identity matrix, the subscripts indicate the time step $k \in \mathbb{N}$. Additionally, \mathbf{S}_d , \mathbf{S}_v and \mathbf{S}_a are the selection matrices for the displacement, velocity and acceleration time series, respectively. Equations (2) and (3) are referred to as process equation and observation equation, respectively.

A special class of dynamical systems concerns cases, for which the external load is an earthquake-induced base excitation. In such a case, a distinction needs to be made between relative and absolute acceleration responses, thereby introducing a modification to the general formulation that has been derived. Specifically, the observation equation can be written as in Eq.(3) but with the direct feedthrough term \mathbf{J} being set to zero. The details of this formulation can be found in [3,13].

2.2 Augmented Kalman Filter (AKF)

The state space formulation derived above, consisting of the process equation (2) and the observation equation (3), can be incorporated into a state estimator, such as the Augmented Kalman Filter (AKF) [7], to simultaneously estimate the state and the unknown input of the system. The state space formulation is rearranged (augmented) via Eq. (4) to favor the simultaneous estimation of both the state and the input for a linear system. Equation (5) corresponds to the observation equation associated with Eq. (4).

$$\mathbf{z}_{k+1}^a = \mathbf{A}^a \mathbf{z}_k^a + \mathbf{w}_k^a \quad (4)$$

$$\mathbf{d}_k = \mathbf{H}_k \mathbf{z}_k^a + \mathbf{v}_k \quad (5)$$

with $\mathbf{z}_k = [\mathbf{y}_k \ \dot{\mathbf{y}}_k \ \mathbf{p}_k]^T$, $\mathbf{A}^a = [\mathbf{A} \ \mathbf{B}; \mathbf{0} \ \mathbf{I}]$ and $\mathbf{H}^a = [\mathbf{H} \ \mathbf{J}]$, where the superscript **a** refers to the augmented state space formulation, \mathbf{w}_k^a and \mathbf{v}_k are the augmented process and measurement noise, both assumed to be zero mean uncorrelated Gaussian noise with covariance matrices $\mathbf{Q}_k^a = \text{block_diag}[\mathbf{Q}_k, \mathbf{S}_k]$ and \mathbf{R}_k^a , respectively. The aim of this study is the optimal calibration of these noise parameters for increasing the reliability of the KF estimation. The detailed AKF algorithm adopted by the current study can be found in [7].

2.3 AKF with time-varying noise parameters

The common practice in input-state estimation using KF methods is to assume that the process and input noise are time-invariant parameters. However, this is not always the case as the modeling uncertainty and the dynamic characteristics of the load may vary in time. Hence, in this work, a methodology is proposed which considers time-variant noise parameters. Specifically, the method is working in conjunction with the AKF and compared to complex optimization schemes, the method pursues via a rather intuitive fashion the identification of the optimal augmented process noise covariance matrix \mathbf{Q}^a for joint input-state estimation. Specifically, the method assumes that the augmented process noise covariance matrix \mathbf{Q}^a is diagonal, with time-varying elements, and relies on the following steps:

- The duration of the dynamic event is divided into N user-defined noise-updating windows. Each of these windows corresponds to a certain amount of analysis time-steps. To simplify the methodology, all windows are assumed to have identical length (i.e., they include the same number of time-steps). The idea is that in each of these windows the noise covariance matrices will be updated.
- The range of values that the diagonal elements of \mathbf{Q} and \mathbf{S} can receive within a specific window is user-defined. However, when no prior knowledge about the system and the input is available, a broad range of values is suggested to be used. For example, it can be assumed that: $10^{-15} \leq \mathbf{Q} \leq 10^{-7}$ and $10^{-5} \leq \mathbf{S} \leq 10^1$, with the diagonal elements of \mathbf{Q} taking values starting from 10^{-15} to 10^{-7} on a logarithmic uniformly distributed scale (i.e., the diagonal elements can be $10^{-15}, 10^{-14}, \dots, 10^{-7}$). The same for the diagonal elements of \mathbf{S} . Hence, within each window, a total of $9 \times 7 = 63$ possible pairs of \mathbf{Q}, \mathbf{S} are available, or, in other words, 63 possible augmented process noise covariance matrices \mathbf{Q}^a .
- For a certain window, and for each of the different \mathbf{Q}^a , state estimation is performed by running the AKF scheme. After the analysis is finished, estimation results have been derived in the examined window from the different augmented process noise covariance matrices. The aim is to identify which of them is the optimal.
- A performance metric is introduced, which can quantify the quality of each estimation. The most reliable metric for this task is considered to be the maximization of the likelihood or the minimization of the negative log-likelihood [3], calculated in Eq. (6) for each \mathbf{Q}^a in the window. In Eq. (6), n_w refers to the number of analysis time-steps in the examined window.
- For the \mathbf{Q}^a that minimizes Eq. (6), the estimated input and state are recovered (i.e., the state vector along with the state error covariance matrix), so that for the next

window the AKF estimation starts from the last estimated state by the optimal filter of the previous window.

- This procedure is repeated until all the windows are finished, providing in this way time-varying noise parameters. A schematic representation of the method is provided in Figure 1.
- The benefit of the method lies in the fact that even when no prior knowledge about the system and the noise covariance matrices (uncertainty of the load and model) exists, the area, where the optimal noise parameters lie, can be readily identified. In addition, given that the different analyses within each window can be performed in parallel, the computational cost may not be prohibitive for large-scale computations.

$$\sum_{k=1}^{n_w} (\log \det \mathbf{s}_k) + \mathbf{e}_k^T \mathbf{s}_k^{-1} \mathbf{e}_k \quad (6)$$

$$\mathbf{e}_k = \mathbf{d}_k - \mathbf{H}_{k-1}^a \mathbf{z}_k^{a-} \quad (7)$$

$$\mathbf{s}_k = \mathbf{H}_{k-1}^a \mathbf{P}_k^{a-} \mathbf{H}_{k-1}^{aT} + \mathbf{R}^a \quad (8)$$

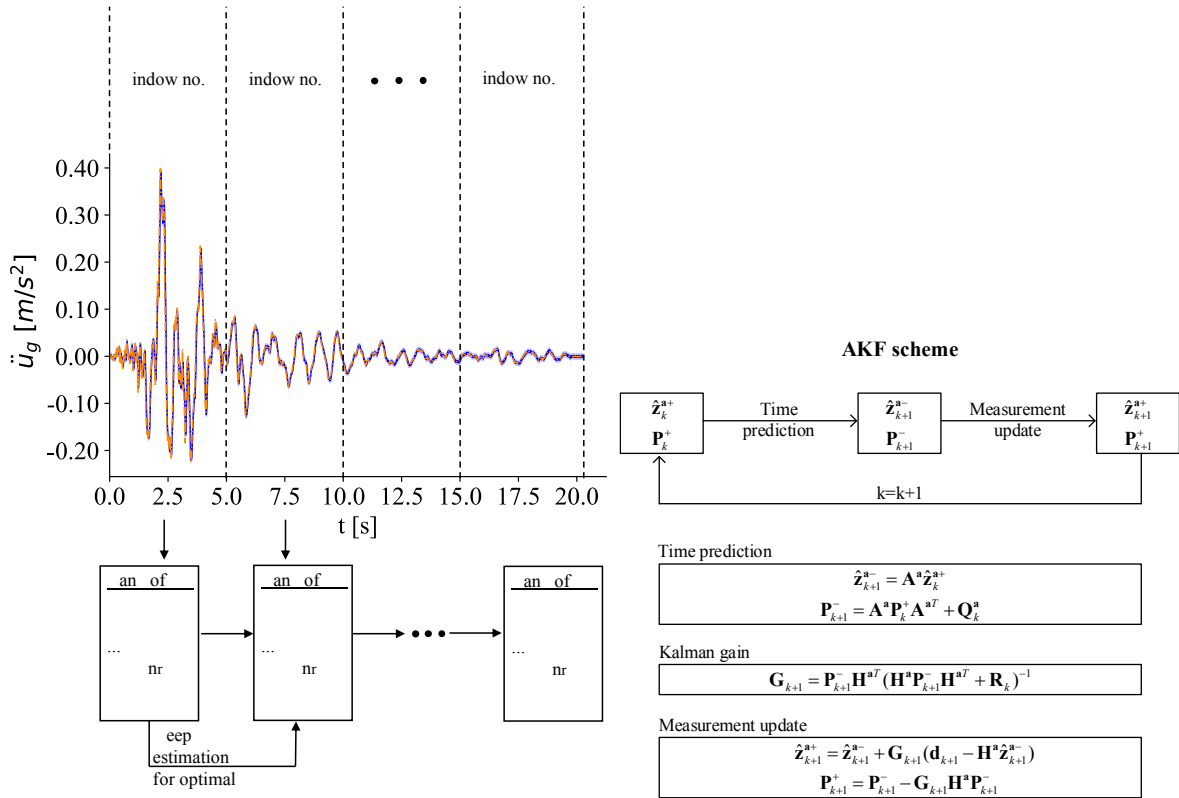


Figure 1: Time-varying noise AKF scheme (left) and filtering equations of the AKF (right). n_r is the number of possible \mathbf{Q} , \mathbf{S} pairs in a window.

2.4 Bayesian Expectation Maximization (BEM) methodology

The BEM methodology [11,12] is also employed in this work for optimal tuning of the noise covariance matrices. The performance of BEM in connection with a larger, more realistic structural system (compared to those in [11,12]) is investigated, and a comparison with the proposed time-varying noise AKF scheme is performed. The details (formulation and computational algorithms) of the BEM method implemented in this work are provided in [11]. It is noteworthy

to mention that, contrarily to the classic EM algorithm that is controlled by the increase in the likelihood function by each iteration, a slightly different objective function, called the surrogate function, is derived in BEM. For the sake of brevity, the derivation of this function is not provided herein but can also be found in [11].

In the calculation of the surrogate function, a computational burden that one may encounter is related to computing the natural logarithm of the determinant of the augmented process noise covariance matrix, namely $\log \det(\mathbf{Q}^a)$. The size of this covariance matrix depends on the size of the FE model, namely the number of its DOFs. The latter implies that for large finite element models, \mathbf{Q}^a will be a square matrix with significantly large dimensions. In such a case, any attempt to calculate the determinant of this covariance matrix will yield such a small value, that eventually most computational tools will consider it as a zero. This happens because the determinants are obtained by multiplication of the elements of the matrix, which are in most cases quite small quantities (e.g., $1e-10$). This further implies that the logarithm cannot be computed, rendering the calculation of the surrogate unfeasible. Ignoring this term is not advised, since it is of high contribution to the surrogate function. To tackle this issue, it is advised to calculate the Cholesky decomposition of the augmented process noise covariance matrix and then directly compute the logarithm as follows:

$$\log \det(\mathbf{Q}^a) = 2 \sum \log \text{diag}(\mathbf{G}) \quad (9)$$

where $\mathbf{G} = \text{chol}(\mathbf{Q}^a)$ is the Cholesky decomposition of the process noise covariance matrix and $\text{diag}(\mathbf{G})$ is the vector of the diagonal elements in \mathbf{G} . It is reminded that the Cholesky decomposition of a matrix can be computed if the matrix is symmetric and positive-definite or positive semi-definite, which is the case for the augmented process noise covariance matrix.

3 NUMERICAL EXAMPLE

The proposed time-varying noise framework, as well as the BEM methodology, will be applied and tested on the basis of a benchmark linear FE model, which is a 2D model of a steel moment resisting frame subjected to earthquake-induced base excitation. Next, a description of the structural system, its FE model as well as the external load and the sensors are provided.

3.1 Model of the 2D steel moment resisting frame

The overall dimensions of the structure and the section profiles of the structural elements, made of steel I and H profiles, are illustrated in Fig. 2 along with the FE model of the structure. At each DOF of the FE model, a translational mass of 12000 kg, along with a rotational mass of $0.0 \text{ g} \cdot \text{m}^2$ are considered. Rayleigh damping, proportional to the mass and to the stiffness, is considered herein while the Rayleigh coefficients are calculated for a damping ratio of 2% for the first and the third modes. No soil-structure interaction is considered in the current study and fixed supports are applied at the base. The modulus of elasticity for steel is $E=210 \text{ GPa}$. The FE model has 60 DOFs and the eigenvalue analysis revealed the following first three periods of the steel structure: 0.994 s, 0.320 s and 0.158 s. Constant gravity loads at the various floor levels are disregarded as they are not considered significant for the investigations within the linear regime. This work is based solely on simulations and the FE model is used to obtain the state-space formulation matrices of the Kalman Filter, as well as for investigating the proposed methods by comparing them with the simulated (true) vibration response of the structure.

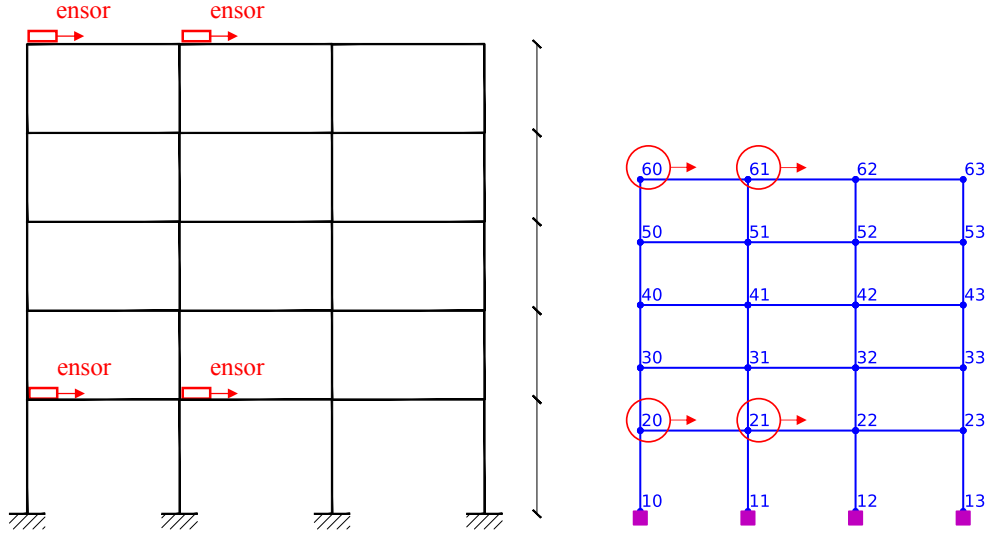


Figure 2: Element cross sections and sensor locations, as well as monitored nodes and dimensions (in m) of the 2D multi-story and multi-bay moment resisting frame studied herein (left). Finite element model with node numbering and sensor locations (right).

3.2 Earthquake load

The methods are tested after subjecting the steel frame to the San Salvador (10/10/86) earthquake. The associated strong ground motion, obtained from the PEER NGA Database, was deliberately reduced after its multiplication with a scale factor equal to 0.1.

3.3 Sensors, measurement noise and initial conditions

Four sensors measuring absolute horizontal accelerations are considered to be available and mounted at the structural system under investigation. In particular, two acceleration time series are assumed to be recorded at the first floor (Sensors 1 and 2 shown in Figure 2) as well as at the top floor (Sensors 3 and 4). All measurements are corrupted with a Gaussian white noise with a standard deviation of 1% of the corresponding clean signal. The sampling period of the measurements is set equal to 0.005 s, which also corresponds to the time step of the simulations. In addition, since gravity loads are ignored, the structure is known to be initially at rest, therefore $\mathbf{z}_0^a = \mathbf{0}$ and $\mathbf{P}_0^a = 10^{-15} \cdot \mathbf{I}_{2n+1}$. Regarding \mathbf{P}_0^a , a sensitivity analysis showed almost negligible impact on the estimation performance in the current study.

4 RESULTS

The current section provides the performance assessment of both the proposed time-varying noise AKF framework and the BEM by comparing the estimated state (i.e., response) quantities with the ones derived directly by numerical analysis of the 2D steel frame system subjected to the chosen earthquake base excitation. Particularly, the assessment of the proposed framework is undertaken herein on the basis of relative displacement and rotation time series. Moreover, the true and estimated unknown input load is also presented. The Time Response Assurance Criterion (TRAC) [14] calculated from both the simulated and the estimated response time series was chosen as a quantitative index of the accuracy related to both the BEM and the time-varying noise AKF estimation of the system's state and input. The TRAC value accounts for the correlation between two time series quantifying their shape-wise similarity or dissimilarity. A perfect match between two time series corresponds to a unit value for the TRAC while its

lower bound is equal to zero. Equation (10) defines the TRAC value between the estimated (indicated with superscript ‘est’) and the corresponding true (derived from time-history analysis of the FE model and indicated with superscript ‘true’) response time series.

$$\text{TRAC} = \frac{[\{y^{\text{est}}(t)\}^T \{y^{\text{true}}(t)\}]^2}{[\{y^{\text{est}}(t)\}^T \{y^{\text{est}}(t)\}] \cdot [\{y^{\text{true}}(t)\}^T \{y^{\text{true}}(t)\}]} \quad (10)$$

The TRAC value was calculated for the relative horizontal displacements and rotations of all the free nodes of the FE model. The vertical DOFs were ignored, since the vertical displacements are extremely small and are not affected significantly by the earthquake motion. Apart from the TRAC-based quantitative assessment of the performance, figures including both the estimated and the true response time series are also shown facilitating a qualitative (visual) assessment. In these figures, the estimation uncertainty bounds are also provided, demonstrating the reliability of the estimation. However, since this study focuses mainly on uncertainty quantification aspects, an additional performance metric is introduced in order to establish a quantitative performance metric for the uncertainty of the estimation. This metric will be called the Uncertainty index (UI) herein. From the AKF algorithm, the mean state estimation along with the corresponding state error covariance matrix are provided at each time step of the simulation. Specifically, the diagonal terms of the state error covariance matrix represent the variance of the mean state estimation (displacement or velocity) at each DOF of the system. Thus, the uncertainty bounds of the AKF estimations can be calculated as $\text{Mean} \pm 2\text{SD}$ (SD stands for standard deviation), which corresponds to a 95% credible interval for the mean. As illustrated in Figure 3, the UI is calculated by first taking the mean value of the 2SD (red vertical lines) above the mean at each time step, and eventually normalizing this quantity by dividing with the standard deviation of the estimated response signal (blue line). The uncertainty index is not bounded by specific values (i.e. the TRAC: $0 \leq \text{TRAC} \leq 1$) and represents a simplified metric for quantifying the extent of the uncertainty bounds. The larger the uncertainty index, the larger are the uncertainty bounds of the estimation. In Eq.(11), the formula for the calculation of the UI is provided:

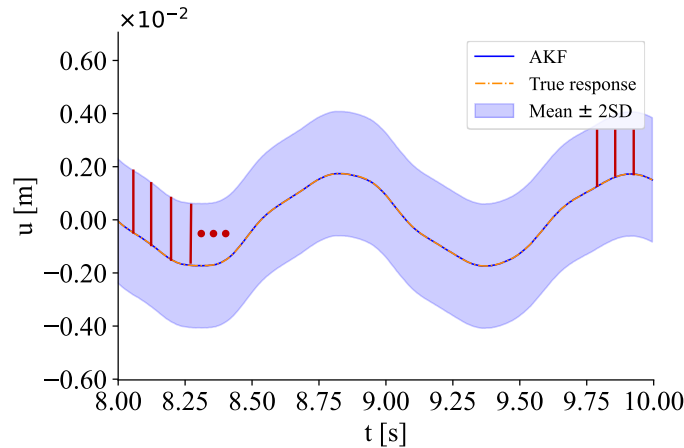


Figure 3: Derivation of the Uncertainty index (UI) metric used herein.

$$\text{UI}_i = \frac{\frac{1}{N} \sum_{k=1}^N 2\sqrt{P_{ii,k}}}{\sigma(\hat{\mathbf{z}}_i)} \quad (11)$$

where $k=1:N$ is the analysis time-step, N is the total number of time-steps, $\sigma(\hat{\mathbf{z}}_i)$ is the standard deviation (SD) of the estimated response $\hat{\mathbf{z}}_i$ by the AKF and $P_{ii,k}$ is the diagonal element of the augmented state error covariance matrix \mathbf{P}_k^a , corresponding to the i^{th} estimated response quantity (displacement or velocity of a certain DOF) of the augmented state vector at time-step k .

4.1 Joint input-state estimation using BEM

First, the BEM method is implemented in order to optimize the augmented process noise covariance matrices and perform the joint input-state estimation for the 2D steel frame subjected to the earthquake-induced base excitation. Specifically, in this numerical example the steady-state BEM algorithm [11] is used as a standalone tool, without employing the main BEM algorithm [11]. The initialization of the BEM algorithm requires setting the initial values of the noise covariance matrices. In this study, \mathbf{R} is defined as a diagonal matrix, whose entries correspond to the true noise measurement signal variances. This is a reasonable assumption as the noise level of the sensors is usually provided by the manufacturer. Specifically, the diagonal elements of \mathbf{R} are in the range of 10^{-7} and 10^{-5} . Regarding the augmented process noise covariance matrices, $\mathbf{Q} = 10^{-8} \cdot \mathbf{I}_{2n}$ and $\mathbf{S} = 10^{-1} \cdot \mathbf{I}_1$ is a scalar since a single unknown external load (base excitation) is considered. Given the presence of multiple local minima, the convergence of the BEM algorithm depends on the initialization, as it happens for any gradient-based optimization scheme. This implies that different sets of initial noise parameters might lead to convergence at different points and affect the performance of the algorithm (e.g. convergence of the algorithm to a local minimum). In the present study, the convergence tolerance of the algorithm is set to 10^{-4} along with a cap of 200 iterations before terminating the algorithm. It needs to be mentioned that BEM results in full covariance matrices, accounting for the correlation between the various DOFs and the different response quantities. To facilitate the assessment of this method, first the estimation results without the use of BEM are provided. Specifically, Figure 4 shows the TRAC and UI values for the case of using only the AKF with $\mathbf{Q} = 10^{-8} \cdot \mathbf{I}_{2n}$ and $\mathbf{S} = 10^{-1} \cdot \mathbf{I}_1$. This set of values represents an average initialization of the noise covariance matrices that leads to very good TRAC values, associated however with significant uncertainty bounds.

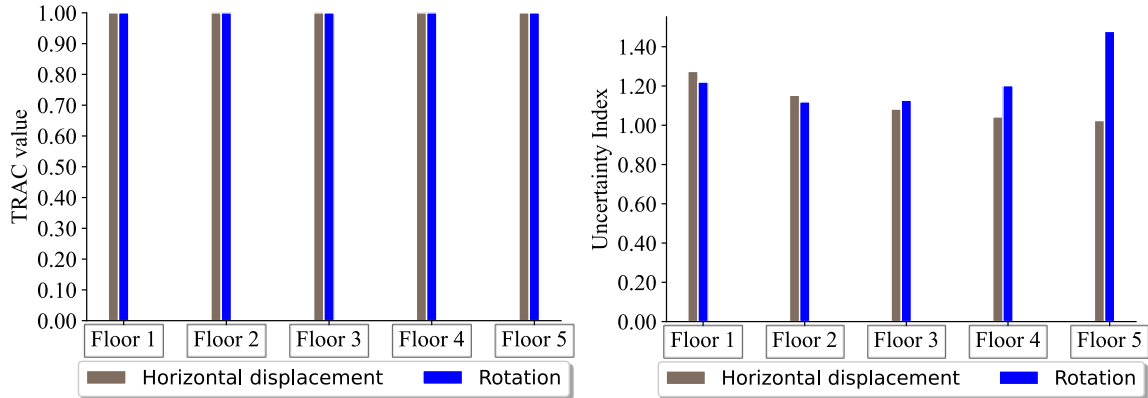


Figure 4: TRAC values quantifying the similarity between the true and the AKF only estimated response at all DOFs averaged per DOF type (i.e., horizontal displacement and rotation) over the nodes of each floor (left). UI values averaged per DOF type over the nodes of each floor (right) for $\mathbf{Q} = 10^{-8} \cdot \mathbf{I}_{2n}$ and $\mathbf{S} = 10^{-1} \cdot \mathbf{I}_1$.

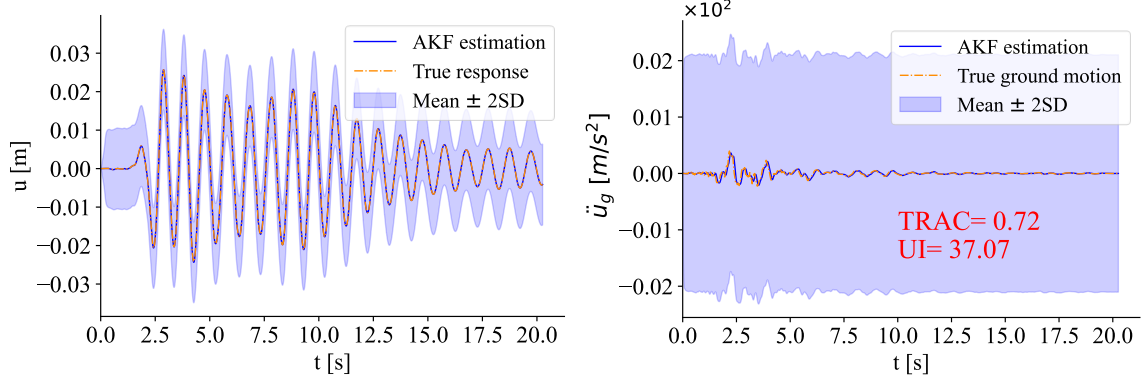


Figure 5: Displacement estimation at the horizontal DOF of node 63 for the case of AKF only (left). Input estimation with TRAC and UI for the case of AKF only (right) for $\mathbf{Q} = 10^{-8} \cdot \mathbf{I}_{2n}$ and $\mathbf{S} = 10^{-1} \cdot \mathbf{I}_1$.

Estimation after use of BEM. Figures 4 and 5 show that, although the initial set of noise parameters leads to excellent TRAC values for the displacements and the load, the corresponding estimation uncertainty is quite significant, especially for the load. The relevant results after the implementation of BEM are summarized in Figures 6 and 7.

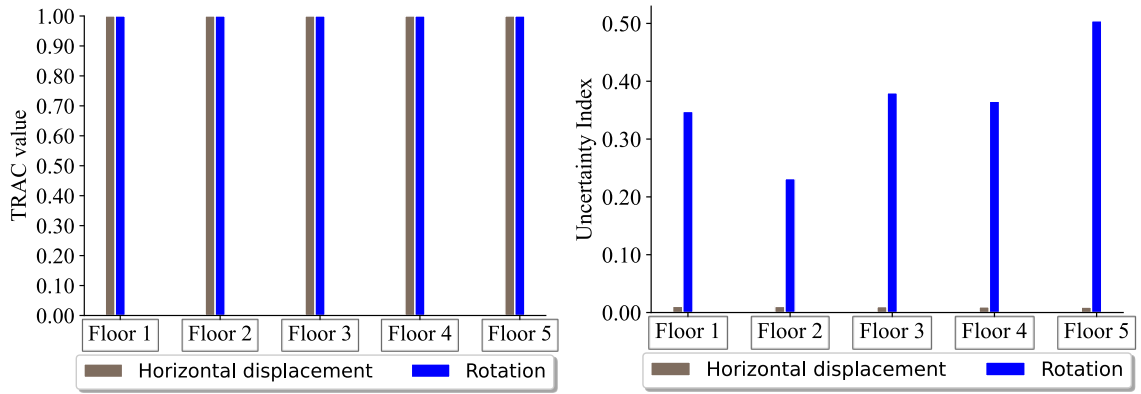


Figure 6: TRAC values (left) and UI values for the BEM estimated response (right).

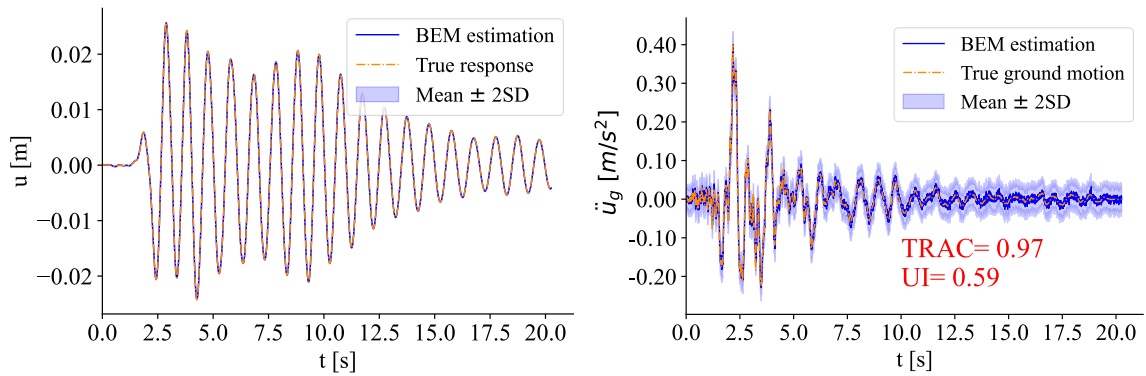


Figure 7: Displacement estimation at horizontal DOF of node 63 after BEM (left). Input estimation with corresponding TRAC and UI values after BEM (right).

It can be seen that the uncertainty of the estimation reduces significantly, and especially for the horizontal DOFs it becomes almost zero. This is due to the sensors measuring horizontal accelerations, and the fact that BEM updates mainly the terms of the process noise covariance matrix

corresponding to horizontal DOFs. Regarding the input estimation, the TRAC becomes almost one and the uncertainty drops remarkably.

4.2 Joint input-state estimation using the time-varying noise AKF

After implementation of BEM, the proposed time-varying noise AKF method is also tested. Contrarily to BEM, this method does not require prior knowledge of the noise covariance matrices since it simply requires a range of possible values for \mathbf{Q} , \mathbf{S} to be defined. Obviously, in case of prior knowledge, this range can be narrowed down, thereby reducing the computational effort. In this study, no prior knowledge is assumed and the range of values mentioned as an example in Section 2 is considered (\mathbf{Q} takes the values 10^{-15} , 10^{-14} ... 0^{-7} , while \mathbf{S} takes 10^{-5} , 10^{-4} ... 10^1 for a total of 63 pairs). To examine the potential of this method and the sensitivity of the estimation to the different number of windows, three distinct cases are considered, with 1, 5 and 50 windows.

Estimation with 1 window. Figures 8 and 9 demonstrate the performance of the method after a single window is used. As can be seen, the TRAC values for the displacements are equal to one and, contrarily to BEM, the uncertainty of the estimation is almost zero for all types of DOFs. In addition, the load is estimated quite well both in terms of mean value and uncertainty.

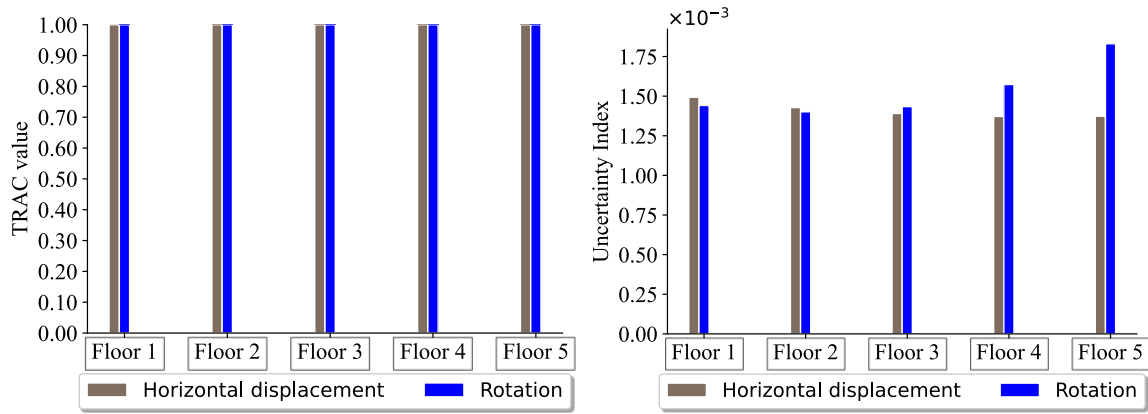


Figure 8: TRAC values (left) and UI values after the time-varying noise AKF with $N=1$ window (right).

After running the 63 Kalman filters within a single window, the selected set of noise parameters was $\mathbf{Q}=10^{-15} \cdot \mathbf{I}_{2n}$ and $\mathbf{S}=10^{-4} \cdot \mathbf{I}_1$. Note that the BEM method converged to the same value for \mathbf{S} (i.e., $1.02 \cdot 10^{-4} \cdot \mathbf{I}_1$) and around 10^{-12} for the diagonal elements of \mathbf{Q} corresponding to the displacements of the horizontal DOFs. On the other hand, the diagonal elements of \mathbf{Q} corresponding to the rotational DOFs, although updated from BEM, remained close to their initial value (i.e., 10^{-8}). Thus, the slightly better performance of this method, mainly in terms of the estimation uncertainty of the rotational DOFs, is attributed to the inability of BEM to significantly update the process noise variances corresponding to the rotational and vertical DOFs, for which no measurements are available. It is noteworthy to mention that the relative comparison of the UI values for the displacement estimations, made by the AKF only, the BEM and the time-varying AKF scheme, is facilitated by the fact that the TRAC values in all three cases are almost the same (Figures 4, 6 and 8). The latter implies that the denominator of Eq.(11) is in all instances identical. This means that the value of the UI depends only on the nominator, which reflects the extent of the uncertainty bounds.

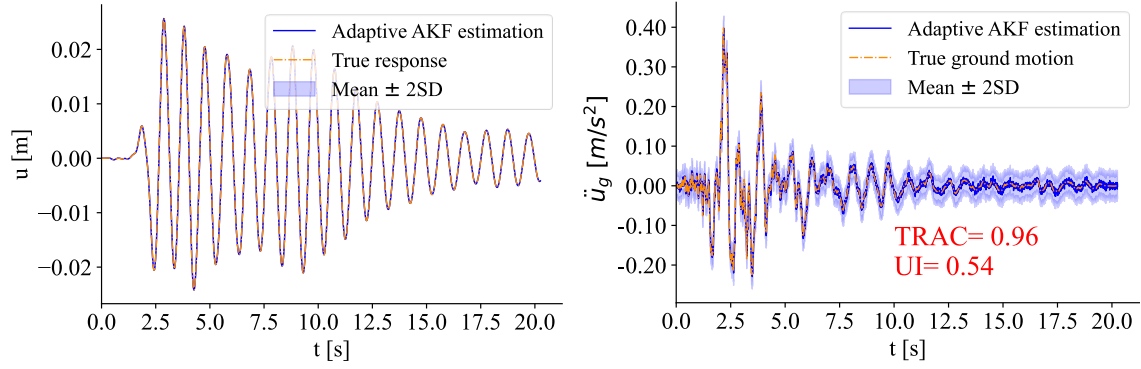


Figure 9: Displacement estimation at horizontal DOF of node 63 after time-varying noise AKF with $N=1$ window (left). Input estimation with corresponding TRAC and UI values after time-varying noise AKF with $N=1$ window (right).

Estimation with 5 and 50 windows. Increasing the number of the noise updating windows leads to a reduction of the uncertainty associated with the load estimation (see Figure 10). The state was already estimated quite confidently even in the case of a single window, thereby the TRAC and UI are not provided again for the sake of brevity. Figure 11 shows the variation of the input noise \mathbf{S} , when either 5 or 50 updating windows are examined. As can be seen, in the case of 50 windows, the variation of \mathbf{S} is bounded by the first 15-17 windows, where the increase in \mathbf{S} happens. The total duration of the earthquake consists of 4052 time-steps with a size of 0.005 seconds. For 50 updating windows this corresponds to a time duration of approximately 0.40 seconds within every window. Hence, the variation of \mathbf{S} mainly happens between the first 7 seconds of the ground motion, which coincides with the true variation of the ground accelerations. It is noted that the process noise \mathbf{Q} , remained constant and equal to $1e-15 \cdot \mathbf{I}_{2n}$ in all windows.

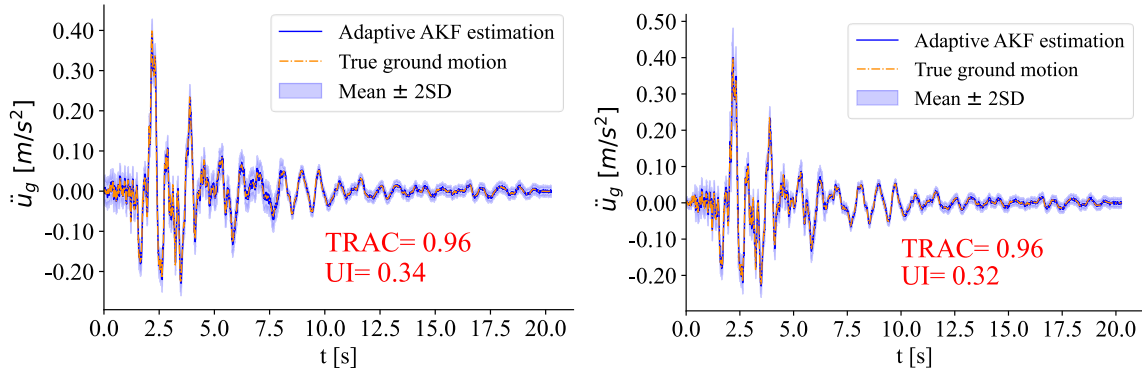


Figure 10: Input estimation with corresponding TRAC and UI values after time-varying noise AKF for $N=5$ windows (left), for $N=50$ windows (right).

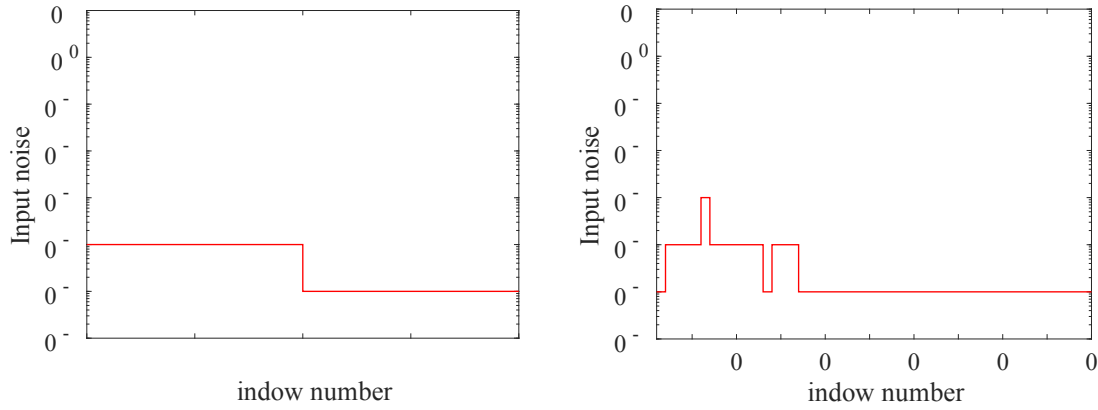


Figure 11: Variation of S in the time-varying noise AKF for $N=5$ windows (left), for $N=50$ windows (right).

5 CONCLUSIONS

This paper focuses on the uncertainty quantification of the joint input-state estimation via Augmented Kalman Filter (AKF) and, in particular, it addresses the tuning of the process and input noise parameters. Two methods have been used in order to tune the parameters, namely a state-of-the-art methodology by Teymouri et al., abbreviated as BEM [11], and a newly developed framework based on adaptive noise covariance matrices. A computational procedure is introduced for BEM, enabling its implementation for large finite element models. Regarding the newly developed framework, it assumes time-varying noise parameters by dividing the whole duration of a dynamic event into noise updating windows. Within each window, multiple Kalman filters can be performed in parallel, each of them corresponding to different values of the process and input noise parameters. Eventually, by evaluating the likelihood of each of these KF estimations, the method selects the optimal pair of noise parameters for input-state estimation in every window. The two methods are tested on a 2D model of a multi-story and multi-bay steel moment resisting frame subjected to an earthquake-induced base excitation. The results show that the time-varying noise AKF has a similar performance to BEM. In addition, compared to BEM, the proposed method shows a reduced response uncertainty associated with rotational DOFs, for which no direct measurement exists. A thorough comparison between the two methods is not feasible, since the estimation made using BEM depends to a certain extent on the initialization of the EM algorithm. Moreover, it is found that the proposed time-varying noise scheme is mainly beneficial for input estimation. A sensitivity study in the number of updating windows showed a reduction in the load estimation uncertainty when more windows are employed. On the contrary, the state was estimated quite well both in terms of mean value and uncertainty even after assuming a single window. In general, it is concluded that both the BEM and the proposed adaptive noise framework can reinforce the reliability of the state estimation. However, the computational effort required in each of the two approaches need to be further investigated. Research is currently dedicated to advance this framework to the nonlinear state estimation.

ACKNOWLEDGEMENTS

The authors would like to acknowledge the Innovation Foundation of Denmark (IFD), which has funded this study via the financial support of the Grand solutions Project titled “Innovative Structural Health Monitoring and Risk Informed Structural Integrity Management (InnoSHM) (0175-00028B).

REFERENCES

- [1] S. E. Azam, E. Chatzi, C. Papadimitriou, A dual Kalman filter approach for state estimation via output-only acceleration measurements. *Mechanical Systems & Signal Processing*, **60**, 866–886, 2015.
- [2] V. K. Dertimanis, E. N. Chatzi, S. E. Azam, C. Papadimitriou, Input-state-parameter estimation of structural systems from limited output information. *Mechanical Systems & Signal Processing*, **126**, 711–746, 2019.
- [3] R. Nayek, S. Chakraborty, S. Narasimhan, A Gaussian process latent force model for joint input-state estimation in linear structural systems. *Mechanical Systems & Signal Processing*, **128**, 497–530, 2019.
- [4] L. Caglio, E. Katsanos, H. Stang, R. Brincker, Structural Damage Detection of Offshore Structures Using Kalman Filtering. *no. Dd. Springer International Publishing*, 2023.
- [5] R. Astroza, H. Ebrahimian, Y. Li, J. P. Conte, Bayesian nonlinear structural FE model and seismic input identification for damage assessment of civil structures. *Mechanical Systems & Signal Processing*, **93**, 661–687, 2017.
- [6] E. Chatzi, C. Papadimitriou, *Identification methods for structural health monitoring*. Springer, 2016.
- [7] E. Lourens, E. Reynders, G. De Roeck, G. Degrande, G. Lombaert, An augmented Kalman filter for force identification in structural dynamics. *Mechanical Systems and Signal Processing*, **27**, 446–460, 2012.
- [8] S. Vettori, E. Di Lorenzo, B. Peeters, M. M. Luczak, E. Chatzi, An adaptive-noise Augmented Kalman Filter approach for input-state estimation in structural dynamics. *Mechanical Systems & Signal Processing*, **184**, 109654, 2023.
- [9] T. Kontoroupi, A. W. Smyth, Online noise identification for joint state and parameter estimation of nonlinear systems. *Journal of Risk and Uncertainty in Engineering Systems, Part A: Civil Engineering*, **2**, B4015006, 2016.
- [10] K.V. Yuen, K.I. Hoi, K.M. Mok, Selection of noise parameters for Kalman filter. *Earthquake Engineering and Engineering Vibration*, **6**, 49-56, 2007.
- [11] D. Teymouri, O. Sedehi, L. S. Katafygiotis, C. Papadimitriou, A Bayesian Expectation-Maximization (BEM) methodology for joint input-state estimation and virtual sensing of structures. *Mechanical Systems & Signal Processing*, **169**, 108602, 2022.
- [12] D. Teymouri, O. Sedehi, L. S. Katafygiotis, C. Papadimitriou, Input-state-parameter-noise identification and virtual sensing in dynamical systems: A Bayesian expectation-maximization (BEM) perspective. *Mechanical Systems & Signal Processing*, **185**, 109758, 2023.
- [13] S. Taher, J. Li, H. Fang, Online input, state, and response estimation for building structures under earthquakes using limited acceleration measurements. *Proc. SPIE 11379, Sensors and Smart Structures Technologies for Civil, Mechanical, and Aerospace Systems 2020*, May 18, 2020.
- [14] P. Avitabile, P. Pingle, Prediction of full field dynamic strain from limited sets of measured data. *Shock and Vibration*, **19**, 765–785, 2012.